J|A|C|S
ARTICLES
Published on Web 04/07/2007

Heterolytic Activation of H−X (X = H, Si, B, and C) Bonds: An Experimental and Theoretical Investigation

C. M. Nagaraja, Pattiyil Parameswaran, Eluvathingal D. Jemmis,* and Balaji R. Jagirdar*

Contribution from the Department of Inorganic & Physical Chemistry, Indian Institute of Science, Bangalore 560 012, India

Received December 18, 2006; E-mail: jagirdar@ipc.iisc.ernet.in

Abstract: The highly electrophilic, coordinatively unsaturated, 16-electron $[Ru(P(OH)_3)(dppe)_2][OTf]_2$ (dppe = $Ph_2PCH_2CH_2PPh_2$) complex **1** activates the H−H, the Si−H, and the B−H bonds, in H_2(g), $EtMe_2SiH$ and Et_3SiH, and $H_3B{\cdot}L$ (L = PMe_3, PPh_3), respectively, in a heterolytic fashion. The heterolysis of H_2 involves an η^2-H_2 complex (observable at low temperatures), whereas the computations indicate that those of the Si−H and the B−H bonds proceed through unobserved η^1-species. The common ruthenium-containing product in these reactions is *trans*-$[Ru(H)(P(OH)_3)(dppe)_2][OTf]$, **2**. The $[Ru(P(OH)_3)(dppe)_2][OTf]_2$ complex is unique with regard to activating the H−H, the Si−H, and the B−H bonds in a heterolytic manner. These reactions and the heterolytic activation of the C−H bond in methane by the model complex $[Ru(POH)_3)(H_2PCH_2CH_2PH_2)_2][Cl][OTf]$, **4**, have been investigated using computational methods as well, at the B3LYP/LANL2DZ level. While the model complex activates the H−H, the Si−H, and the B−H bonds in H_2, SiH_4, and $H_3B{\cdot}L$ (L = PMe_3, PPh_3), respectively, with a low barrier, activation of the C−H bond in CH_4 involves a transition state of 57.5 kcal/mol high in energy. The inability of the ruthenium complex to activate CH_4 is due to the undue stretching of the C−H bond needed at the transition state, in comparison to the other substrates.

Introduction

The binding of molecular hydrogen to a metal center and its subsequent activation either toward homolysis or heterolysis has been intensively studied.[1] Electron-donating ligands on the metal center enhance the M → H_2 back-donation, resulting in the oxidative addition of dihydrogen to a metal center. On the other hand, H_2 bound to electron-deficient or highly electrophilic metal centers results in reduced back-donation from the metal to the dihydrogen. This is, however, offset by an increased σ-donation from the H_2 to the metal. In such a scenario, heterolytic activation of the dihydrogen ligand to generate a proton and a metal hydride takes place. The heterolytic splitting of H_2 bound to electron-rich neutral metal complexes is usually brought about by strong bases. However, when H_2 is bound to highly electrophilic metal centers, its tendency to undergo heterolysis tremendously increases.[1a,b] Both homolysis and heterolysis of H_2 are important chemical reactions and have been identified in catalytic hydrogenation reactions. In addition to the binding and heterolysis of the H−H bond in H_2, the σ-coordination and the heterolytic activation of X−H (X = Si, B) bonds of other molecules such as silanes and borane−Lewis base adducts have close resemblances to those of H_2 and are quite significant because they serve as models for the activation and functionalization of the C−H bond of methane and other alkanes. The partial oxidation of methane in natural gas to a liquid fuel, for example, methanol, is one of the holy grails in the field of catalysis.[2]

There have been several reports of highly acidic dihydrogen complexes in the literature.[3] The heterolytic splitting of Si−H bond has also been observed by many.[4] However, only three systems are known to bring about the heterolytic activation of H−H and Si−H bonds in a parallel fashion.[4e,f,i] Complexes that bring about the heterolysis of the B−H bond in boranes/borane−Lewis base adducts are very few in number.[5] Although no experimental evidence is available, heterolytic cleavage of the C−H bond of methane could be expected to take place in the Shilov-type chemistry[6] for the conversion of methane into methanol using a "superelectrophilic" Pt(II) complex.[7] Recently,

(1) (a) Kubas, G. J. *Adv. Inorg. Chem.* **2004**, *56*, 127−177. (b) Kubas, G. J. *Metal Dihydrogen and σ-Bond Complexes*; Kluwer Academic: New York, 2000. (c) Peruzzini, M., Poli, R., Eds. *Recent Advances in Hydride Chemistry*; Elsevier: Amsterdam, 2001.

(2) Arndtsen, B. A.; Bergman, R. G.; Mobley, T. A.; Peterson, T. H. *Acc. Chem. Res.* **1995**, *28*, 154−162.

(3) (a) Nanishankar, H. V.; Nethaji, M.; Jagirdar, B. R. *Eur. J. Inorg. Chem.* **2004**, 3048−3056. (b) Majumdar, K. K.; Nanishankar, H. V.; Jagirdar, B. R. *Eur. J. Inorg. Chem.* **2001**, 1847−1853. (c) Landau, S. E.; Morris, R. H.; Lough, A. J. *Inorg. Chem.* **1999**, *38*, 6060−6068. (d) Kubas, G. J.; Huhmann-Vincent, J.; Scott, B. L. *Inorg. Chem.* **1999**, *38*, 115−124. (e) Fong, T. P.; Forde, C. E.; Lough, A. J.; Morris, R. H.; Rigo, P.; Rocchini, E.; Stephan, T. *J. Chem. Soc., Dalton Trans.* **1999**, 4475−4486. (f) Huhmann-Vincent, J.; Scott, B. L.; Kubas, G. J. *J. Am. Chem. Soc.* **1998**, *120*, 6808−6809. (g) Ontko, A. C.; Houlis, J. F.; Schnabel, R. C.; Roddick, D. M.; Fong, T. P.; Lough, A. J.; Morris, R. H. *Organometallics* **1998**, *17*, 5467−5476. (h) Rocchini, E.; Mezzetti, A.; Ruegger, H.; Burckhardt, U.; Gramlich, V.; Del Zotto, A.; Martinuzzi, P.; Rigo, P. *Inorg. Chem.* **1997**, *36*, 711−720. (i) Schlaf, M.; Lough, A. J.; Maltby, P. A.; Morris, R. H. *Organometallics* **1996**, *15*, 2270−2278. (j) Morris, R. H. *Can. J. Chem.* **1996**, *74*, 1907−1915. (k) Keady, M. S.; Koola, J. D.; Ontko, A. C.; Merwin, R. K.; Roddick, D. M. *Organometallics* **1992**, *11*, 3417−3421. (l) Jia, G.; Morris, R. H. *J. Am. Chem. Soc.* **1991**, *113*, 875−883. (m) Chinn, M. S.; Heinekey, D. M.; Payne, N. G.; Sofield, C. D. *Organometallics* **1989**, *8*, 1824−1826.

Periana et al.[8] observed catalytic H/D exchange with methane in the presence of a cyclometalated Pt(II)-substituted bipyridine complex. However, their theoretical studies suggest that the C−H cleavage barrier was high. Density functional study of the C−H bond activation in methane using model complexes of the type [M(CH$_3$)(HN═CHCH═NH)] (M = Pd$^+$, Pt$^+$, Rh$^+$, Ir$^+$, Rh, Ir) by Swang et al.[9] suggest that oxidative addition is favored except for Pd$^+$ and Rh$^+$. Despite the metal center being electrophilic in the case of certain third-row metal complexes, the oxidative addition and heterolytic cleavage pathways are close in energy, depending on the ancillary ligand environment, the charge, and the reaction conditions.

For the accomplishment of heterolysis of X−H (X = H, Si, B, C) bonds, the requirement of a "superelectrophilic" metal center has been suggested as a necessity.[1a,b] To our knowledge, there are no examples in the literature of a single system that has the ability to bring about the heterolysis of all of these bonds. With a view to realize such a system, we recently prepared and characterized a stable, 16-electron, coordinatively unsaturated, "superelectrophilic" ruthenium complex [Ru(P(OH)$_3$)(dppe)$_2$][OTf]$_2$, **1**, that cleaves the H−H bond in hydrogen gas in a heterolytic fashion.[10] Herein, we report the results of our findings on the heterolytic cleavage reactions of X−H (X = H, Si, B, C) bonds using complex **1**. With a view to get an insight into the factors that dictate the heterolytic cleavage pathway for these bonds, we carried out density functional study of the activation of X−H (X = H, Si, B, C) bonds using a model complex [Ru(P(OH)$_3$)(H$_2$PCH$_2$CH$_2$PH$_2$)$_2$][Cl][OTf], **4**. The results of these studies are also presented.

Experimental Section

General Procedures. All of the reactions were carried out under an atmosphere of dry and oxygen-free N_2 at room temperature using standard Schlenk and inert atmosphere techniques unless otherwise specified.[11] The ^{1}H, ^{31}P, ^{13}C, and ^{11}B NMR spectral data were obtained using an Avance Bruker 400 MHz instrument. The ^{31}P NMR spectra were recorded relative to 85% H_3PO_4 (aqueous solution) as an external standard. Variable-temperature ^{1}H T_1 measurements were carried out at 400 MHz using the inversion recovery method.[12] High-pressure NMR tubes fitted with Swage-lock fittings were procured from Wilmad Glass. Methane gas (99.95%) was obtained from Bhoruka Gases Limited, Bangalore, India, and $^{13}CH_4$ (99.8 atom %) was from Sigma-Aldrich. The silanes Me$_2$EtSiH, Et$_3$SiH, and Ph$_3$SiH were purchased from Sigma-Aldrich and used as received. The borane−Lewis base adducts H$_3$B·PPh$_3$ and H$_3$B·PMe$_3$ were prepared by passing B_2H_6 gas through toluene solutions containing the respective phosphines.[13] The *trans*-[Ru(H)(η^2-H$_2$)(dppe)$_2$][OTf][14] and [Ru(P(OH)$_3$)(dppe)$_2$][OTf]$_2$,[10] **1**, complexes were prepared using literature procedures. Note: Wherever the term head gas has been used, it means that the gas was introduced on top of the solution and the solution was either shaken or stirred.

Reaction of [Ru(P(OH)$_3$)(dppe)$_2$][OTf]$_2$, 1, with H_2 (Head Gas) at 298 K. Complex **1** (0.020 g, 0.015 mmol) was dissolved in 0.6 mL of Ar-saturated CD_2Cl_2 in a septum-capped 5 mm NMR tube. Next, H_2 (1 atm) was introduced as a head gas for a period of 5 min. The ^{1}H and the ^{31}P NMR spectra of the sample recorded immediately thereafter at 298 K showed the formation of a mixture of *trans*-[Ru(H)(P(OH)$_3$)(dppe)$_2$][OTf], **2** (70%), and *trans*-[Ru(H)(η^2-H$_2$)(dppe)$_2$][OTf] (30%) complexes. ^{1}H NMR of **2** (298 K, CD_2Cl_2): δ −8.90 (d qnt, 1H, Ru−*H*, *J*(H, P$_{trans}$) = 107.0 Hz, *J*(H, P$_{cis}$) = 20.0 Hz), 2.36 (m, 4H, C*H*$_2$), 2.86 (m, 4H, C*H*$_2$), 7.00−7.60 (m, 40H, P(C$_6$*H*$_5$)$_2$). ^{31}P{^{1}H}NMR (CD_2Cl_2): δ 66.5 (d, 4P, *P*CH$_2$CH$_2$*P*, *J*(P, P$_{cis}$) = 32.0 Hz), 137.3 (qnt, 1P, *P*(OH)$_3$). ^{1}H NMR of *trans*-[Ru(H)(η^2-H$_2$)(dppe)$_2$][OTf] (298 K, CD_2Cl_2): δ −10.13 (qnt, 1H, Ru−*H*, *J*(H, P$_{cis}$) = 17.5 Hz), −4.78 (br s, 2H, Ru−*H*$_2$), 2.17 (m, 8H, C*H*$_2$), 6.78−7.79 (m, 40H, P(C$_6$*H*$_5$)$_2$). ^{31}P-{^{1}H} NMR (CD_2Cl_2): δ 68.7 (s, 4P, *P*CH$_2$CH$_2$*P*).

Reaction of 1 with H_2 (Head Gas) at 223 K − Observation of *trans*-[Ru(η^2-H$_2$)(P(OH)$_3$)(dppe)$_2$][OTf]$_2$, 3. Complex **1** (0.020 g, 0.015 mmol) was dissolved in 0.6 mL of Ar-saturated CD_2Cl_2 in a septum-capped 5 mm NMR tube. The tube was cooled to 203 K. Next, H_2 gas (1 atm) was introduced as a head gas for a period of 5−10 min at 203 K; immediately the sample was inserted into the NMR probe, which was pre-cooled to 223 K. The ^{1}H and ^{31}P NMR spectra recorded at 223 K showed the presence of the dihydrogen complex **3**. ^{1}H NMR of **3** (223 K, CD_2Cl_2): δ −5.47 (br s, 2H, Ru−*H*$_2$), 2.80 (m, 4H, C*H*$_2$), 3.32 (m, 4H, C*H*$_2$), 7.00−7.60 (m, 40H, P(C$_6$*H*$_5$)$_2$). ^{31}P{^{1}H} NMR (CD_2Cl_2): δ 53.5 (d, 4P, *P*CH$_2$CH$_2$*P*, *J*(P, P$_{cis}$) = 41.0 Hz), 113.4 (qnt, 1P, *P*(OH)$_3$). Variable-temperature ^{1}H spin−lattice relaxation times at 400 MHz, T_1 (ms) (temperature, K): 27.4 (203), 24.5 (213), 21.6 (223), 17.3 (233), 14.4 (243).

Reaction of 1 with HD (Head Gas) at 223 K − Preparation of *trans*-[Ru(η^2-HD)(P(OH)$_3$)(dppe)$_2$][OTf]$_2$, 3-*d*. Complex **1** (0.020 g, 0.015 mmol) was dissolved in 0.6 mL of Ar-saturated CD_2Cl_2 in a septum-capped 5 mm NMR tube. The tube was maintained at 203 K. HD gas (generated from NaH and D_2O) was introduced at 203 K as a head gas for a period of 5−10 min. Immediately thereafter, the sample was inserted into the NMR probe that was pre-cooled to 223 K. The HD isotopomer *trans*-[Ru(η^2-HD)(P(OH)$_3$)(dppe)$_2$][OTf]$_2$, **3-*d***, formed was characterized by ^{1}H NMR spectroscopy at 223 K. The residual signal due to the H_2 complex was nullified using an inversion recovery pulse.

Reaction of 1 with Silanes (Me$_2$EtSiH, Et$_3$SiH, Ph$_3$SiH). All of these reactions were carried out in a similar manner. Complex **1** (0.020 g, 0.015 mmol) was dissolved in 0.6 mL of CD_2Cl_2 in a 5 mm NMR tube. The resulting solution was degassed, and then 1 equiv of silane (1.9 μL, 0.015 mmol (Me$_2$EtSiH); 2.4 μL, 0.015 mmol (Et$_3$SiH); 0.004 g, 0.015 mmol (Ph$_3$SiH)) was added at 77 K, and the tube was sealed under vacuum. The sample was slowly warmed to 298 K and then

(4) (a) Pool, J. A.; Lofkovsky, E.; Chirik, P. J. *Nature* **2004**, *427*, 527−530. (b) Vincent, J. L.; Luo, S.; Scott, B. L.; Butcher, R.; Unkefer, C. J.; Burns, C. J.; Kubas, G. J.; Lledos, A.; Maseras, F.; Tomas, J. *Organometallics* **2003**, *22*, 5307−5323. (c) Llamazares, A.; Schmalle, H. W.; Berke, H. *Organometallics* **2001**, *20*, 5277−5288. (d) Fang, X.; Scott, B. L.; Watkin, J. G.; Kubas, G. J. *Organometallics* **2000**, *19*, 4193−4195. (e) Fang, X.; Scott, B. L.; John, K. D.; Kubas, G. J. *Organometallics* **2000**, *19*, 4141−4149. (f) Huhmann-Vincent, J.; Scott, B. L.; Kubas, G. J. *Inorg. Chim. Acta* **1999**, *294*, 240−254. (g) Basch, H.; Muaev, D. G.; Morokuma, K.; Fryzuk, M. D.; Love, J. B.; Seidel, W. W.; Albinati, A.; Koetzle, T. F.; Klooster, W. T.; Mason, S. A.; Eckert, J. *J. Am. Chem. Soc.* **1999**, *121*, 523−528. (h) Sweeney, Z. K.; Polse, J. L.; Andersen, R. A.; Bergman, R. G.; Kubinec, M. G. *J. Am. Chem. Soc.* **1997**, *119*, 4543−4544. (i) Fryzuk, M. D.; Love, J. B.; Rettig, S. J.; Young, V. G. *Science* **1997**, *275*, 1445−1447. (j) Luo, X. L.; Kubas, G. J.; Bryan, J. C.; Burns, C. J.; Unkefer, C. J. *J. Am. Chem. Soc.* **1994**, *116*, 10312−10313. (k) Luo, X. L.; Crabtree, R. H. *J. Am. Chem. Soc.* **1989**, *111*, 2527−2535.

(5) (a) Kawano, Y.; Hashiva, M.; Shimoi, M. *Organometallics* **2006**, *25*, 4420−4426. (b) Yasue, T.; Kawano, Y.; Shimoi, M. *Angew. Chem., Int. Ed.* **2003**, *42*, 1727−1730.

(6) Shilov, A. E.; Shul'pin, G. B. *Chem. Rev.* **1997**, *97*, 2879−2932.

(7) Periana, R. A.; Taube, D. J.; Gamble, S.; Taube, H.; Satoh, T.; Fujii, H. *Science* **1998**, *280*, 560−564.

(8) Young, K. J. H.; Meier, S. K.; Gonzales, J. M.; Oxgaard, J.; Goddard, W. A., III; Periana, R. A. *Organometallics* **2006**, *25*, 4734−4737.

(9) Heiberg, H.; Gropen, O.; Swang, O. *Int. J. Quantum Chem.* **2003**, *92*, 391−399.

(10) Nagaraja, C. M.; Nethaji, M.; Jagirdar, B. R. *Inorg. Chem.* **2005**, *44*, 4145−4147.

(11) (a) Shriver, D. F.; Drezdon, M. A. *The Manipulation of Air Sensitive Compounds*, 2nd ed.; Wiley: New York, 1986. (b) Herzog, S.; Dehnert, J.; Luhder, K. In *Technique of Inorganic Chemistry*; Johnassen, H. B., Ed.; Interscience: New York, 1969; Vol. VII.

(12) Hamilton, D. G.; Crabtree, R. H. *J. Am. Chem. Soc.* **1988**, *110*, 4126−4133.

(13) Hewitt, F.; Holliday, A. K. *J. Chem. Soc.* **1953**, 530−534.

(14) Bautista, M. T.; Cappellani, E. P.; Drouin, S. D.; Morris, R. H.; Schweitzer, C. T.; Sella, A.; Zubkowski, J. *J. Am. Chem. Soc.* **1991**, *113*, 4876−4887 (this reference reports the preparation of the BF_4 salt).

inserted into the NMR probe maintained at 298 K. The ^{1}H and ^{31}P NMR spectra were recorded at intervals of 30 min over a period of 15 h.

Reaction of 1 with Boranes ($H_3B{\cdot}PMe_3$, $H_3B{\cdot}PPh_3$). Complex **1** (0.020 g, 0.015 mmol) and slightly more than 1 equiv of $H_3B{\cdot}L$ (L = PMe_3 (0.002 g, 0.022 mmol), PPh_3 (0.005 g, 0.018 mmol)) were taken in a 5 mm NMR tube. The tube was evacuated for ca. 6−8 h. Next, THF (0.6 mL) (acetone-d_6 external lock) was cannula transferred into the tube under vacuum at 203 K. The tube was dropped into the NMR probe that was pre-cooled to 223 K. The progress of the reaction was monitored by recording the ^{1}H, the ^{31}P, and the ^{11}B NMR spectra of the sample over a temperature range 223−323 K.

Reaction of 1 with Methane (4 bar). Complex **1** (0.050 g, 0.038 mmol) was dissolved in 2 mL of CH_2Cl_2 in a 250 mL thick-walled Pyrex glass bottle. To this solution was added 10 equiv (6.8 μL, 0.380 mmol) of deionized water. The reaction mixture was degassed, and then CH_4 (4 bar) was introduced. The bottle was continuously shaken, and the progress of the reaction was monitored using NMR spectroscopy. The ^{1}H NMR spectrum of an aliquot recorded after 3 h of reaction showed the presence of a small amount of the hydride complex **2**. The reaction was monitored for 10−15 h using NMR spectroscopy; no change in the signal intensity of the hydride ligand was apparent with time. Although the experiment was repeated several times, the hydride complex was observed only a few times (5 out of 20 runs). The conditions under which the hydride complex was obtained could not be established with certainty, and, therefore, the experiment could not be reproduced.

Reaction of 1 with Methane (4 bar) in a High-Pressure NMR Tube. Complex **1** (0.020 g, 0.015 mmol) was dissolved in 0.6 mL of CD_2Cl_2 in a high-pressure NMR tube. 10 equiv of deionized water (2.7 μL, 0.150 mmol) was added. The solution was subjected to three freeze−pump−thaw degassing cycles, and then CH_4 (4 bar) was introduced into the tube. The tube was then sealed off, and the progress of the reaction was monitored using NMR spectroscopy. ^{1}H NMR spectroscopy did not reveal the formation of the hydride complex **2**.

Computational Details. All of the calculations were performed using the Gaussian 03[15] program at the B3LYP[16] level of theory, which consists of a hybrid Becke+Hartree−Fock exchange and Lee−Yang−Parr correlation functional with nonlocal correlations. The basis set used is LANL2DZ.[17] All of the reactants, products, intermediates, and transition states were optimized without any symmetry restrictions and were identified by the number of imaginary vibrational frequencies. The total energies (au), zero point energies (kcal/mol), and the number of imaginary vibrational frequencies of the model complex **4**, reactants, the intermediates **5a**−**5d**, the transition states (**5a(TS)**−**5d(TS)**), and the products are summarized in Table S1 (see Supporting Information). The reaction coordinates were followed by the intrinsic reaction coordinate (IRC) technique.[18] A model complex [Ru(P(OH)$_3$)($H_2PCH_2CH_2PH_2$)$_2$][Cl][OTf], **4**, was used for the calculation. One of the counterions [OTf]$^-$ was replaced with a Cl$^-$ to reduce the computation time in locating the transition states. The general reaction for the computations is shown in Scheme 4. To understand the effect of solvent on the relative energies, we carried out single point calculation on the optimized geometries at the B3LYP/LANL2DZ level using the polar continuum model (PCM) with dichloromethane (dielectric constant, ϵ = 8.93) as a solvent.[19] We also optimized all structures at the BP86/ZORA/TZP level using the ADF05.01 package.[20] BP86 includes the exchange functional of Becke[16a,b] and the correlation functional of Predew.[21] The basis sets for all of the atoms here are of triple-ζ quality having one set of polarization functions for all atoms. Zero-order regular approximation (ZORA) implemented in ADF05.01 is used to account for relativistic effects.[22] There is no major change in the relative energies at this level; the discussion is based on the results from the B3LYP/LANL2DZ level unless otherwise specified.

Results and Discussion

Heterolytic Activation of H_2. Free H_2 is a very weak acid with a pK_a of ca. 35 in THF.[23] However, when it is bound to a highly electrophilic cationic metal center, the acidity increases drastically. When the 16-electron, coordinatively unsaturated, dicationic ruthenium complex [Ru(P(OH)$_3$)(dppe)$_2$][OTf]$_2$, **1**, was exposed to an atmosphere of H_2 gas at 298 K, HOTf, a very strong acid, is spontaneously obtained. This is accompanied by the formation of a mixture of hydride complexes *trans*-[Ru(H)(P(OH)$_3$)(dppe)$_2$][OTf], **2** (70%), and *trans*-[Ru(H)(η^2-H_2)(dppe)$_2$][OTf] (30%) (formed by the substitution of P(OH)$_3$ with H_2). The HOTf is hydrogen bonded to the [OTf]$^-$ counterion of the hydride complex (**2**), which was detected using NMR spectroscopy as has been done before by Morris et al.[3e] The generation of HOTf and the hydride complex (**2**) proceeds via the intermediacy of the dihydrogen complex, *trans*-[Ru(η^2-H_2)(P(OH)$_3$)(dppe)$_2$][OTf]$_2$, **3**. Lledós et al.[24] studied the effect of pairing of the homoconjugate ions on the metal hydride protonation and concluded that the stability of the dihydrogen bonding between the proton source and metal hydride depends on the basicity of the hydride. The dihydrogen complex (**3**) is quite acidic (see discussion later) and can be stabilized only in the presence of an excess of HOTf, suggesting that the heterolysis of H_2 to give the metal hydride complex and HOTf formation are more favorable than the reverse reaction. In addition, we found that the hydride complex (**2**) can only be protonated using HOTf; no protonation occurs with acids weaker in strength than HOTf. To observe the complex **3**, **1** was treated with H_2 (head gas) at 203 K. The ^{1}H NMR spectrum at 203 or 223 K shows a broad singlet at δ −5.47 for the η^2-H_2 ligand. The ^{31}P NMR spectrum exhibits a doublet at δ 53.5 for the dppe phosphorus due to the coupling with P(OH)$_3$ and a quintet at δ 113.4 for the P(OH)$_3$ phosphorus with a J(P, P_{cis}) of 41.0 Hz. Upon raising the temperature of the sample, the intensity of the H_2 signal decreases and that of the hydride increases, indicating the heterolysis of the bound H_2; at 253 K, the dihydrogen complex is completely transformed into the hydride **2**. The VT ^{1}H NMR spectral stack plot of the hydride region for this reaction is shown in Figure 1. The heterolysis of H_2 can take place via several mechanisms with or without the involvement of a dihydrogen complex. A frequent problem is the difficulty in identification of the involvement of a dihydrogen

(15) Frisch, M. J.; et al. *Gaussian 03*, revision C.02; Gaussian, Inc.: Wallingford, CT, 2004.
(16) (a) Becke, A. D. *J. Chem. Phys.* **1993**, *98*, 5648−5652. (b) Becke, A. D. *Phys. Rev. A* **1988**, *38*, 3098−3100. (c) Lee, C.; Yang, W.; Parr, R. G. *Phys. Rev. B* **1988**, *37*, 785−789.
(17) Hay, P. J.; Wadt, W. R. *J. Chem. Phys.* **1985**, *82*, 299−310.
(18) Fukui, K.; Kato, S.; Fujimoto, H. *J. Am. Chem. Soc.* **1975**, *97*, 1−7.
(19) (a) Miertus, S.; Scrocco, E.; Tomasi, J. *Chem. Phys.* **1981**, *55*, 117−129. (b) Miertus, S.; Tomasi, J. *Chem. Phys.* **1982**, *65*, 239−245. (c) Cossi, M.; Barone, V.; Cammi, R.; Tomasi, J. *Chem. Phys. Lett.* **1996**, *255*, 327−335.
(20) (a) *ADF2005.01*; SCM, Theoretical Chemistry, Vrije Universiteit: Amsterdam, The Netherlands, http://www.scm.com. (b) te Velde, G.; Bickelhaupt, F. M.; Baerends, E. J.; Fonseca Guerra, C.; van Gisbergen, S. J. A.; Snijders, J. G.; Ziegler, T. *J. Comput. Chem.* **2001**, *22*, 931−967. (c) Fonseca Guerra, C.; Snijders, J.; te Velde, G.; Baerends, E. J. *Theor. Chem. Acc.* **1998**, *99*, 391−403.
(21) Perdew, J. P. *Phys. Rev. B* **1986**, *33*, 8822−8824.
(22) (a) Snijders, J. G.; Baerends, E. J. *Mol. Phys.* **1978**, *36*, 1789−1804. (b) Snijders, J. G.; Baerends, E. J.; Ros, P. *Mol. Phys.* **1979**, *38*, 1909−1929.
(23) Buncel, B.; Menon, B. *J. Am. Chem. Soc.* **1977**, *99*, 4457−4461.
(24) (a) Belkova, N. V.; Collange, E.; Dub, P.; Epstein, L. M.; Lemenovskii, D. A.; Lledós, A.; Maresca, O.; Maseras, F.; Poli, R.; Revin, P. O.; Shubina, E. S.; Vorontsov, E. V. *Chem.-Eur. J.* **2005**, *11*, 873−888. (b) Belkova, N. V.; Besora, M.; Epstein, L. M.; Lledós, A.; Maseras, F.; Shubina, E. S. *J. Am. Chem. Soc.* **2003**, *125*, 7715−7725.

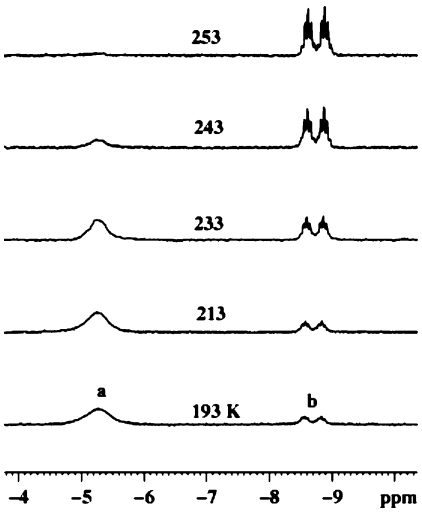

Figure 1. Hydride region of the variable-temperature ^{1}H NMR (CD_2Cl_2, 400 MHz) spectral stack plot for the reaction of [Ru(P(OH)$_3$)(dppe)$_2$][OTf]$_2$, **1**, and H_2 (head gas): (a) *trans*-[Ru(η^2-H$_2$)(P(OH)$_3$)(dppe)$_2$][OTf]$_2$, **3**, (b) *trans*-[Ru(H)(P(OH)$_3$)(dppe)$_2$][OTf], **2**.

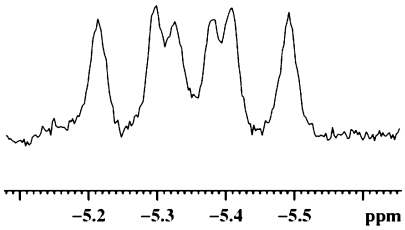

Figure 2. ^{1}H NMR spectrum (243 K, CD_2Cl_2, 400 MHz) of the hydride region of *trans*-[Ru(η^2-HD)(P(OH)$_3$)(dppe)$_2$][OTf]$_2$, **3**-*d*.

(M−η^2-H$_2$) (and/or dihydride, M(H)$_2$) complex. In our case, we have been able to identify both spectroscopically as well as theoretically (see later) the involvement of a dihydrogen complex (M−η^2-H$_2$, **3**). We also carried out VT ^{1}H spin−lattice relaxation time measurements of complex **3** at 400 MHz. In the temperature range 203−243 K, a T_1 (min) could not be found. However, the short T_1 values (see Experimental Section) qualitatively indicate the intact nature of the H−H bond in **3**. To unequivocally establish the identity of the dihydrogen complex, we treated **1** with HD gas (generated from NaH and D_2O) at 193 K. The ^{1}H NMR spectrum of this sample at 213 K in the hydride region shows an approximate doublet of 1:1:1 triplets pattern (Figure 2). Because there is some overlap of signals, a perfect doublet of 1:1:1 triplet was not observed. The doublet is due to HD−P$_{trans}$ coupling of 44.0 Hz. We have observed such large couplings earlier.[25] The 1:1:1 triplet is due to J(H, D) of 33.3 Hz. The H−H distance (d_{HH} Å) calculated from the inverse relationship between d_{HH} and J(H, D) is 0.86 Å.[26] It is typical of acidic dihydrogen complexes to exhibit high values of J(H, D) for their η^2-HD isotopomers; however, the pK_a's do not correlate well with J(H, D).[1a,b] The positive charge and electron-withdrawing co-ligands, in particular the one trans to the bound H_2, significantly increase the acidity. Our attempts to measure the pK_a of **3** failed because, even at 193 K, we

Scheme 1. Heterolysis of H_2 in the Presence of a Lewis Base by [Ru(P(OH)$_3$)(dppe)$_2$][OTf]$_2$, **1**, and Its Regeneration from *trans*-[Ru(H)(P(OH)$_3$)(dppe)$_2$][OTf], **2**, Complex

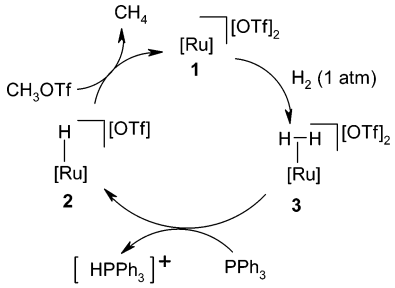

observed heterolysis of the bound H_2 and the appearance of a small quantity of the hydride complex (**2**) in the ^{1}H NMR spectrum. The fact that complex **1** is a dicationic, formally 16-electron ruthenium center with a P(OH)$_3$ group suggests that the corresponding dihydrogen complex **3** will be extremely acidic. Although we do not have the pK_a value of the dihydrogen complex **3**, it must be comparable to that of the isostructural ruthenium complexes *trans*-[Ru(CNH)(η^2-H$_2$)(dppe)$_2$]$^{2+}$, *trans*-[Ru(CNH)(η^2-H$_2$)(dppp)$_2$]$^{2+}$,[3e,27] (dppp = Ph$_2$PCH$_2$CH$_2$CH$_2$-PPh$_2$), and *trans*-[Ru(CO)(η^2-H$_2$)(dppp)$_2$]$^{2+}$.[3h] It is notable that complex **1** is one of the very few examples of dihydrogen complexes with highly acidic η^2-H$_2$ that is generated directly from H$_2$(g).[3e−g,4f,27,28]

Introduction of H_2 gas to a solution containing complex **1** and PPh_3 resulted in the formation of the hydride complex **2** and [HPPh$_3$]$^+$, which is evident from the ^{31}P{^{1}H} NMR signal at δ 2.2 (free PPh_3: δ −5.6). Complex **1** can be regenerated quantitatively simply by the treatment of the hydride complex **2** with MeOTf. This reaction is accompanied by methane evolution (Scheme 1).

At this juncture, it is pertinent to compare the properties of complex **1** and those of Kubas' rhenium complex, *cis*-[Re(CO)$_4$-(PR$_3$)(CH$_2$Cl$_2$)][BAr$_F$].[3f] The CH_2Cl_2 is labile and can be displaced by H$_2$(g), which undergoes heterolysis. The pK_a of this complex was estimated to be about −2. With a d_{HH} of ∼0.87 Å, which is consistent with the bonding picture of the dihydrogen complexes possessing highly electrophilic metal centers, the metal−H$_2$ σ interaction is a lot stronger than the back-bonding interaction. We found that complex **1** is remarkably stable toward air and moisture in the solid state as well as in solution. This is in stark contrast to what is expected of a coordinatively unsaturated, 16-electron complex with a dicationic metal center. We also found that complex **1** does not react with water.[29] Unlike in Morris' ruthenium complex, *trans*-[Ru-(OTf)(CNH)(dppe)$_2$][OTf],[3e] wherein a triflate counterion binds to the metal, the two triflate counterions remain free in complex **1**. The P(OH)$_3$ moiety is actively hydrogen bonded to the triflate counterions, stabilizing the five-coordinate species.[10] Efforts in our laboratory are in progress to explore the utility of complex

(25) (a) Mathew, N.; Jagirdar, B. R.; Gopalan, R. S.; Kulkarni, G. U. *Organometallics* **2000**, *19*, 4506−4517. (b) Mathew, N.; Jagirdar, B. R. *Inorg. Chem.* **2000**, *39*, 5404−5406.

(26) (a) Maltby, P. A.; Schlaf, M.; Steinbeck, M.; Lough, A. J.; Morris, R. H.; Klooster, W. T.; Koetzle, T. F.; Srivastava, R. C. *J. Am. Chem. Soc.* **1996**, *118*, 5396−5407. (b) d_{HH} (Å) = −0.0167[J(H, D) (Hz)] + 1.42.

(27) Fong, T. P.; Lough, A. J.; Morris, R. H.; Mezzetti, A.; Rocchini, E.; Rigo, P. *J. Chem. Soc., Dalton Trans.* **1998**, 2111−2114.

(28) Highly acidic η^2-H$_2$ generated directly from H$_2$(g): refs 3e−g, 4f, and 27. (a) Gilbertson, J. D.; Szymczak, N. K.; Tyler, D. R. *Inorg. Chem.* **2004**, *43*, 3341−3343. (b) Bianchini, C.; Moneti, S.; Peruzzini, M.; Vizza, F. *Inorg. Chem.* **1997**, *36*, 5818−5825.

(29) Complex **1** (0.020 g, 0.015 mmol) was dissolved in CD_2Cl_2, and 10 equiv (2.8 μL, 0.15 mmol) of H_2O was added. The reaction was monitored by both ^{1}H and ^{31}P{^{1}H} NMR spectroscopy. No change in the spectral properties of complex **1** was noted even after 2 days.

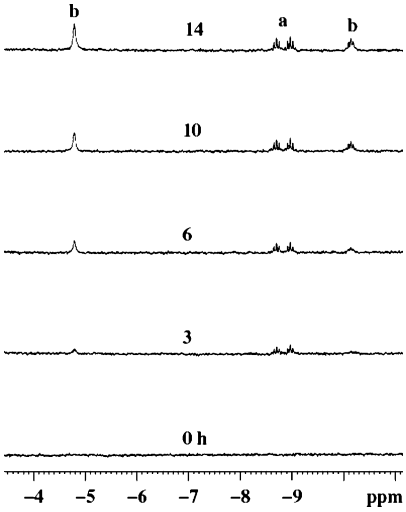

Figure 3. Hydride region of the time-elapsed ^{1}H NMR (CD_2Cl_2, 400 MHz) spectral stack plot for the reaction of [Ru(P(OH)$_3$)(dppe)$_2$][OTf]$_2$, **1**, and Me_2EtSiH: (a) *trans*-[Ru(H)(P(OH)$_3$)(dppe)$_2$][OTf], **2**, (b) *trans*-[Ru(H)-(η^2-H$_2$)(dppe)$_2$][OTf].

1 for the heterolysis of H_2 in the solid phase by anchoring it onto a suitable support.

Heterolytic Cleavage of Si−H Bond. The Si−H bond in silanes can bind to the metal fragments and forms stable σ complexes via 3c−2e bonds. When the Si−H moiety is coordinated to an electrophilic metal center, the positive charge on Si increases, favoring its effective elimination as R_3SiOTf. Brookhart et al.[30] noted that cationic η^2-silane complexes are quite sensitive to weak nucleophiles or even non-nucleophilic counterions such as BF_4^-, resulting in the formation of R_3SiF. The binding of Si−H bond to a metal center and its subsequent activation has close resemblance to that of H_2 and other σ-bonded complexes. Hence, the silane serves as a model for the activation and functionalization of C−H bonds in alkanes, in particular, CH_4.[1b]

Reaction of complex **1** with Me_2EtSiH at 298 K gave the hydride complex **2** within 2 h of reaction time. After ca. 5 h, NMR spectroscopy showed the formation of the dihydrogen/hydride complex *trans*-[Ru(H)(η^2-H$_2$)(dppe)$_2$][OTf]. These changes are shown in Figure 3. The formation of the hydride complex (**2**) should proceed through the intermediacy of a σ-complex involving either an η^1-Si−H or an η^2-Si−H species. We could not observe the σ-complex spectroscopically. However, our theoretical studies (see later) suggest an intermediate involving an η^1-Si−H complex in the heterolysis of silane using a model complex similar to **1**. The η^1-Si−H complex is a short-lived species that undergoes heterolysis to give the hydride and the silylium cation, $[Me_2EtSi]^+$, which is eliminated as Me_2-EtSiOTf. We measured the heterolytic cleavage rates of the reaction as a function of the steric bulk of the silane. Triphenylsilane did not react in a 1:1 mixture of metal complex and Ph_3SiH. However, similar ratios of reagents gave a rate constant $k = 3.8 \times 10^{-4}$ s^{-1} for Me_2EtSiH and $k = 2.6 \times 10^{-4}$ s^{-1} for Et_3SiH. This suggests that the coordination of the silane to the metal center is an important step before the bond activation can take place. Ph_3SiH, being very bulky, cannot approach the vacant site of the metal center.

As is evident from Figure 3, with time, the concentration of **2** builds up. In addition, another hydride complex, *trans*-[Ru(H)(η^2-H$_2$)(dppe)$_2$][OTf], is also formed. Silane heterolysis involves the generation of a very reactive silylium cation that will interact with the triflate counterion to form silyl triflate. Silyl triflate is hydrophilic in nature and reacts with adventitious water, resulting in the formation of a silanol accompanied by the release of a proton equivalent that protonates the hydride complex (**2**) to give the corresponding dihydrogen complex (**3**). The H_2 ligand eventually is eliminated, and, when a sufficient concentration of free H_2 is established, the P(OH)$_3$ moiety of the hydride complex, *trans*-[Ru(H)(P(OH)$_3$)(dppe)$_2$][OTf], gets displaced by the free H_2, resulting in the formation of the dihydrogen/hydride complex, *trans*-[Ru(H)(η^2-H$_2$)(dppe)$_2$][OTf]. There is precedence for the abstraction of OH^- from adventitious water by silylium cation.[31] When the reaction of complex **1** and Et_3SiH was carried out in a thoroughly dried NMR tube and very dry solvent, we did not observe the formation of the dihydrogen/hydride complex (see Supporting Information). This reactivity is summarized in Scheme 2.

Scheme 2. Heterolytic Activation of the Si−H Bond in Silanes Using [Ru(P(OH)$_3$)(dppe)$_2$][OTf]$_2$, **1**

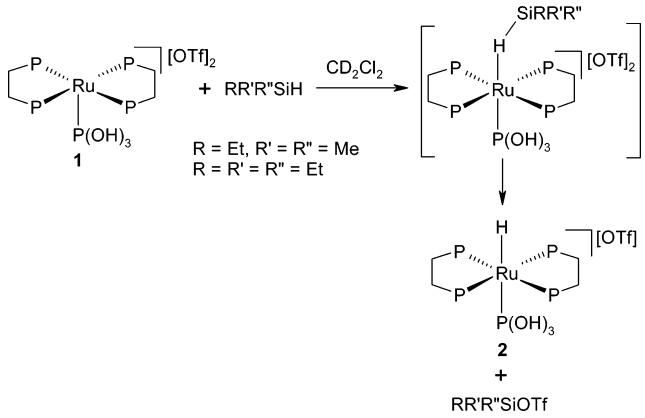

The heterolysis of silanes by electrophilic cationic metal complexes, especially those of manganese, rhenium, iridium, palladium, and platinum, has been reported.[4b,d,e,j,k] In all of the reported systems, a combination of different ligands that drain the electron density from the metal to make it more electrophilic is present. In addition, the silane is bound in an η^2-fashion to the metal in all of those cases. In both respects, our complex differs from the rest: complex **1** has all phosphorus co-ligands, and the silane is η^1-bound to the metal. The steric congestion of the diphosphine ligands on the metal center allows approach of molecules such as silanes, boranes, and methane (see later) in such a way that they are forced to bind to the metal center in an η^1-fashion only.

Electron-donating substituents on silicon decrease the Si−H interaction with the metal center, fostering σ binding over homolysis. On the other hand, electron-withdrawing substituents on Si promote homolysis due to enhanced back-donation.[1a] However, the interaction of a silane with highly electrophilic fragments with electron-withdrawing groups on the metal, for example, $Cr(CO)_5$, is an exception to these generalizations.[32] In this case, the metal−silane binding strength decreases with

(30) Scharrer, E.; Chang, S.; Brookhart, M. *Organometallics* **1995**, *14*, 5686−5694.
(31) Fang, X.; Huhmann-Vincent, J.; Scott, B. L.; Kubas, G. J. *J. Organomet. Chem.* **2000**, *609*, 95−103.
(32) Zhang, S.; Dobson, G. R.; Brown, T. L. *J. Am. Chem. Soc.* **1991**, *113*, 6908−6916.

Scheme 3. Heterolysis of the B−H Bond in Borane−Lewis Base Adducts Using $[Ru(P(OH)_3)(dppe)_2][OTf]_2$, **1**

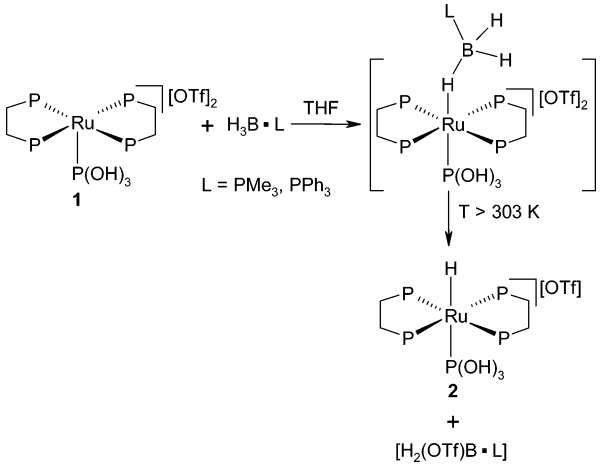

more electron-withdrawing groups on silicon, which reflects the increased importance of Si−H → M σ donation in relation to the back-donation component. Heinekey recently reported silane complexes of the type $[M(CO)_5(\eta^2\text{-HSiEt}_3)]$ (M = Cr, Mo, W).[33] In our system, which is a 16-electron, coordinatively unsaturated, dicationic metal center, although we have not been able to observe the silane complex, the σ-binding must be strong with almost negligible back-donation from the metal to the σ^* orbital of SiH. Our theoretical studies (see later) show a very modest Si−H bond elongation on coordination, which is consistent with this postulate.

Heterolytic Cleavage of B−H Bond. The coordination and the subsequent activation of the B−H bond of monoborane−Lewis base adducts $H_3B{\cdot}L$ (L = neutral Lewis base), which are isoelectronic with alkanes, serve as models for the activation and functionalization of the C−H bond of alkanes. Theoretical calculations on the nature of the interaction of the B−H bond of borane with a metal center suggest that the BH σ-binding with the metal d(σ) orbital predominates, whereas the high energy of the BH σ^* orbital significantly limits the back-donation.[34,35] Thus, when a borane adduct is bound to an electrophilic metal center, the electron density from the borane is drained effectively by the metal. Consequently, the M−H interaction becomes quite strong, whereas the B−H bond weakens, driving the heterolytic cleavage of the B−H bond.

Reaction of complex **1** with $H_3B{\cdot}L$ (L = PMe_3, PPh_3) at 203 K did not show any apparent spectral changes. Upon warming the sample to 303 K, the ^{1}H NMR spectrum showed the formation of the hydride complex **2**. Heating the sample to 323 K increases the intensity of the hydride signal and decreases that of the free borane (^{11}B NMR of $H_3B{\cdot}PMe_3$, δ −35.6 (q d, J(B, H) = 95.0 Hz, J(B, P) = 56.0 Hz)); $H_3B{\cdot}PPh_3$, δ −33.0 (q d, J(B, H) = 92.0 Hz, J(B, P) = 63.0 Hz)). In addition, the ^{11}B NMR spectrum showed a new broad resonance (δ 22.0, br mult ($H_3B{\cdot}PMe_3$)); δ 23.8, br s ($H_3B{\cdot}PPh_3$). These new signals are attributed to $H_2(OTf)B{\cdot}PMe_3$ and $H_2(OTf)B{\cdot}PPh_3$, respectively, indicating that the B−H bond has been cleaved in a heterolytic fashion. The $^{31}P\{^1H\}$ NMR spectrum showed a singlet at δ −1.28 for $H_2(OTf)B{\cdot}PPh_3$. Although we were unable to observe the intermediate, our theoretical studies propose that the heterolysis of the B−H bond proceeds via the intermediacy of an η^1-borane metal complex (see later) (Scheme 3). The $^{31}P\{^1H\}$ and ^{11}B NMR spectral stack plots of this reaction as a function of temperature are shown in Figures 4 and 5, respectively.

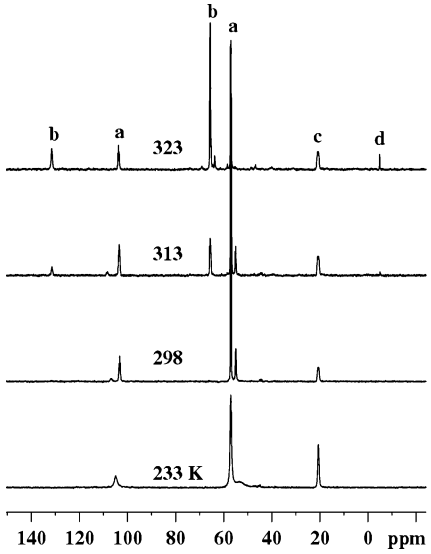

Figure 4. Variable-temperature $^{31}P\{^1H\}$ NMR (CD_2Cl_2, 400 MHz) spectral stack plot for the reaction of $[Ru(P(OH)_3)(dppe)_2][OTf]_2$, **1**, and $H_3B{\cdot}PPh_3$: (a) $[Ru(P(OH)_3)(dppe)_2][OTf]_2$, **1**, (b) *trans*-$[Ru(H)(P(OH)_3)(dppe)_2][OTf]$, **2**, (c) $H_3B{\cdot}PPh_3$, (d) $H_2(OTf)B{\cdot}PPh_3$.

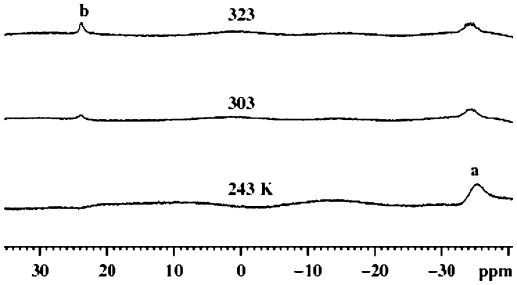

Figure 5. Variable-temperature ^{11}B NMR (CD_2Cl_2, 400 MHz) spectral stack plot for the reaction of $[Ru(P(OH)_3)(dppe)_2][OTf]_2$, **1**, and $H_3B{\cdot}PPh_3$: (a) free $H_3B{\cdot}PPh_3$, (b) $H_2(OTf)B{\cdot}PPh_3$.

Shimoi et al.[5b] reported a σ-borane complex, $[Mn(CO)_4(PR_3)(\eta^1\text{-}H_3B{\cdot}PMe_3)]^+$, which undergoes decomposition in solution at room temperature via the heterolysis of the bound borane to give the manganese hydride complex and $[H_2B{\cdot}2PMe_3]^+$. Theoretical calculations on a model complex show that the hydrogen of the borane moiety becomes more hydridic upon coordination to the metal center, facilitating the heterolysis of the B−H bond. This is a characteristic feature of cationic systems, whereas the neutral borane complexes eliminate borane exclusively. In addition to Shimoi's complexes, Weller et al. recently reported certain ruthenium complexes wherein the borane adducts are η^1-bound to the metal.[36] In our system, the heterolysis of the borane adduct takes place, resulting in the hydride complex (**2**) and $H_2(OTf)B{\cdot}L$ (L = PMe_3, PPh_3).

(33) Heinekey, D. M.; Matthews, S. L.; Pons, V. *Inorg. Chem.* **2006**, *45*, 6453−6459.
(34) Shimoi, M.; Nagai, S.; Ichikawa, M.; Kawano, Y.; Katoh, K.; Uruichi, M.; Ogino, H. *J. Am. Chem. Soc.* **1999**, *121*, 11704−11712.
(35) Kakizawa, T.; Kawano, Y.; Shimoi, M. *Organometallics* **2001**, *20*, 3211−3213.
(36) (a) Merle, N.; Frost, C. G.; Kociok-Köhn, G.; Willis, M. C.; Weller, A. S. *J. Organomet. Chem.* **2005**, *690*, 2829−2834. (b) Merle, N.; Kociok-Köhn, G.; Mahon, M. F.; Frost, C. G.; Ruggerio, G. D.; Weller, A. S. *Dalton Trans.* **2004**, 3883−3892.

Attempted Heterolytic Activation of the C−H Bond of Methane. One of our prime research interests is to prepare stable and isolable alkane complexes of transition metals and the attendant partial oxidation of the C−H bond of alkanes, especially methane, in the hope of realizing methane conversion catalysts to generate methanol. Although stable σ complexes of H_2, silanes, and boranes, which have a close overall relationship with alkanes, have been isolated, alkane σ complexes of transition metals are still elusive except for $[M(CO)_5(alkane)]$ (M = Cr, Mo, W),[37] $[MnCp(CO)_2(alkane)]$,[38] and $[ReCp(CO)_2(alkane)]$.[39] We explored the potential of complex **1** toward the heterolytic activation of methane.

Reaction of complex **1** with CH_4 (4 bar) at 298 K in a high-pressure reactor was carried out, and the reaction was monitored by NMR spectroscopy. An aliquot of the reaction mixture after 3 h did not show any apparent change in the spectral characteristics from the initial ones. If the C−H bond heterolysis indeed took place, we could expect the formation of the hydride complex **2** and MeOTf. Because MeOTf abstracts the hydride from complex **2** to give back complex **1** (Scheme 1), the reaction was carried out in the presence of 10 equiv of deionized water to hydrolyze the MeOTf into MeOH. In this experiment, we observed small quantities of the hydride complex **2** (ca. 5−10%) in the ^{1}H NMR spectrum. We repeated this experiment several times, and, surprisingly, only five experiments (out of 20 runs) gave the above results. The pathway of this reaction or the source of the hydride hydrogen in the preparative scale experiments is unclear. The source of the hydride hydrogen could be from the H_2 impurity in CH_4(g) (99.95% used for our experiments), which is below the detectable limits of the NMR spectrometer. This cannot be ruled out. Reaction of complex **1** with $^{13}CH_4$ (4 bar) in the presence of water in a high-pressure NMR tube gave no hydride complex **2**.

The Pt(II)-catalyzed methane to methanol conversion reported by Periana et al. most likely involves the heterolysis of the C−H bond of methane because the metal center is cationic and highly electrophilic.[7] Although no direct experimental evidence is available for this heterolytic cleavage, the C−H bond activation involving H/D exchange between acidic protons in η^2-C−H agostic systems and bases such as water and methanol by electrophilic complexes is known.[40] Tilset and co-workers recently reported reversible intramolecular heterolytic C−H activation at diazabutadiene ligands on an Ir(III) center.[41]

Computational Studies. The definite variations in the reactivity of H_2, R_3SiH, $H_3B{\cdot}L$ (L = PMe_3, PPh_3), and CH_4 with complex **1** prompted us to study the details of the transition states and energetics computationally. The main goal of the computational study is to compare the reactivity of the different X−H σ bonds with the electrophilic metal center in $[Ru(P(OH)_3)(dppe)_2][OTf]_2$, **1**. A model complex $[Ru(P(OH)_3)(H_2PCH_2CH_2PH_2)_2][OTf][Cl]$, **4**, was used for the computations, and the reaction scheme shown in Scheme 4 was assumed. One of the counterions $[OTf]^-$ was replaced with a Cl^- to reduce the computation time in locating the transition states. The initial complexes with H_2, SiH_4, $H_3B{\cdot}PH_3$, and CH_4 were characterized as minima (**5a**−**5d**), and the transition states (**5a(TS)**−**5d(TS)**) were characterized with one imaginary vibrational frequency. To understand the effect of counterions for stabilization of the initial intermediate, we have optimized the structures **5b** and **5c** by removing their counterions. Even though there is a considerable variation in the geometrical parameters, their energy minima on the potential energy surface show that the counterions do not have a major role in stabilizing these η^1-coordinated complexes (see Supporting Information). Similarly, we have used both of the counterions as triflate ions to check the variations in the relative energies (see Supporting Information). The relative trend in the reaction energies is almost similar.

Scheme 4. Model Reaction for the Heterolytic Activation of the H−X (X = H, SiH_3, $H_2B{\cdot}PH_3$, and CH_3) Bonds Using $[Ru(P(OH)_3)(H_2PCH_2CH_2PH_2)_2][OTf][Cl]$, **4**

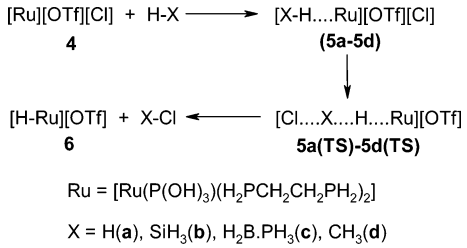

As shown in the reaction scheme, the initial complex, **5a**−**5d**, goes to the products, **6** and X−Cl, through the transition state **5a(TS)**−**5d(TS)**. The optimized structures at B3LYP/LANL2DZ level of theory are shown in Figure 6. To understand the effect of solvent on the relative stabilities of the different geometries, we have carried out single point calculations on the gas-phase optimized geometries at the B3LYP/LANL2DZ level of theory using polarizable continuum models (PCM) with parameters corresponding to dichloromethane (experimentally used, dielectric constant, ϵ = 8.93). Because the dichloromethane stabilizes all of the geometries in a similar manner, it does not alter the relative stabilities significantly (see Supporting Information). There is no major change in the relative energies at the BP86/ZORA/TZP level of theory as well (see Supporting Information).

Activation of the H−H Bond. Molecular hydrogen can bind nearly as well to electron-rich metal fragments that oxidatively add H_2 to give the dihydride as to very electron-deficient metal centers, which are weak back donors. The reduction in back-donation in highly electrophilic metal complexes is nearly completely compensated by an increased σ-donation from H_2 to an empty metal d-orbital. The presence of a highly electrophilic metal fragment induces a shift of electron density from H_2 to the metal, making both the hydrogens slightly positive, and hence the bound H_2 becomes highly acidic. The intermediate structure (**5a**, Figure 6) having an H_2 bound to the ruthenium atom in an η^2-H_2 fashion has the two hydrogen atoms equidistant from ruthenium at 1.820 Å. The H−H bond distance of 0.818 Å indicates an elongation of 0.075 Å from a value of 0.743 Å in free H_2.[42,43] This modest elongation (10%) is a reflection of

(37) (a) Graham, M. A.; Poliakoff, M.; Turner, J. J. *J. Chem. Soc. A* **1971**, 2939−2948. (b) Sun, X. Z.; Grills, D. C.; Nikiforov, S. M.; Poliakoff, M.; George, M. W. *J. Am. Chem. Soc.* **1997**, *119*, 7521−7525. (c) Zaric, S.; Hall, M. B. *J. Phys. Chem. A* **1997**, *101*, 4646−4652.

(38) (a) Klassen, J. K.; Selke, M.; Sorensen, A. A.; Yang, G. K. *J. Am. Chem. Soc.* **1990**, *112*, 1267−1268. (b) Johnson, F. P. A.; George, M. W.; Bagratashvili, V. N.; Vereshchagina, L. N.; Poliakoff, M. *Mendeleev Commun.* **1991**, 26−28.

(39) (a) Geftakis, S.; Ball, G. E. *J. Am. Chem. Soc.* **1998**, *120*, 9953−9954. (b) Lawes, D. J.; Geftakis, S.; Ball, G. E. *J. Am. Chem. Soc.* **2005**, *127*, 4134−4135.

(40) Rybtchinski, B.; Cohen, R.; Ben-David, Y.; Martin, J. M. L.; Milstein, D. *J. Am. Chem. Soc.* **2003**, *125*, 11041−11050.

(41) Wik, B. J.; Romming, C.; Tilset, M. *J. Mol. Catal. A: Chem.* **2002**, *189*, 23−32.

(42) Free H_2 molecule has been optimized at the same level of theory (B3LYP/LANL2DZ). The H−H distance thus obtained is 0.744 Å.

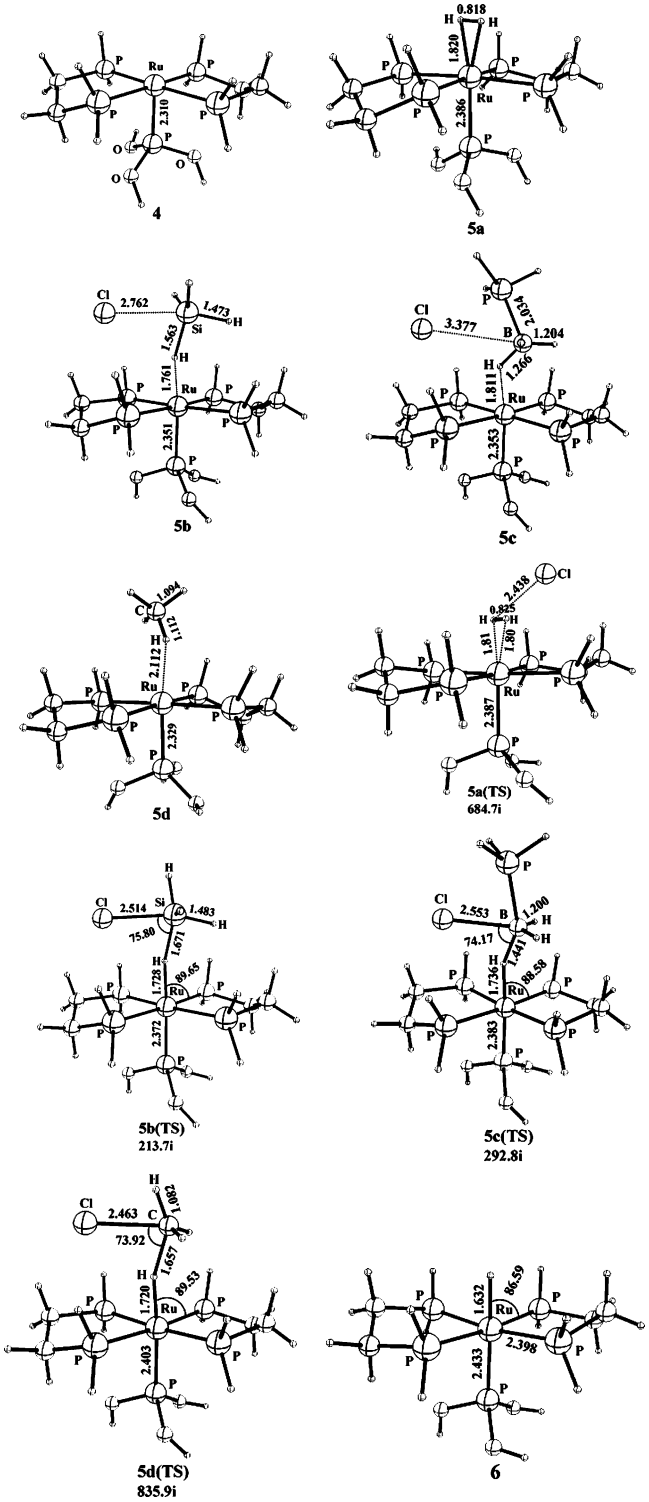

Figure 6. B3LYP/LANL2DZ-optimized structures (bond lengths and angles in angstroms and degrees) of the reactant **4**, intermediates (**5a**−**5d**), transition states (**5a(TS)**−**5d(TS)**) (the imaginary frequencies in cm^{-1} are also given), and the product **6**. The $[OTf]^-$ (and Cl^- in some cases) that is H-bonded to the $P(OH)_3$ ligand has been omitted for clarity in the figures. The optimized structures of the free molecules (reactants and products) are given in the Supporting Information.

the high electrophilicity of the ruthenium center. The corresponding elongation at the BP86/ZORA/TZP level of theory is

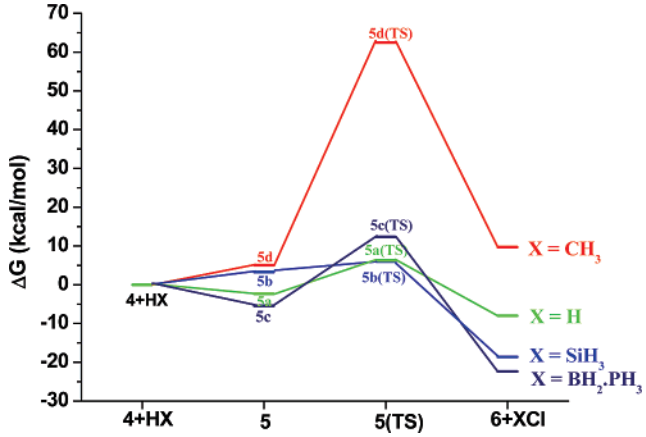

Figure 7. Potential energy diagram of the activation of the H−X (X = H, SiH_3, $H_2B{\cdot}PH_3$, CH_3) bonds using the model complex **4**. The free energies relative to reactants are presented.

14.5%. The d_{HH} estimated from the experimental J(H, D) is 0.86 Å, not much different from the one obtained from theory. An interaction diagram (see Supporting Information) clearly shows the dominance of the σ bonding between the H_2 and the metal center; however, the estimation of charge transfer precisely was rendered difficult due to the close proximity of one of the counterions Cl^- to the H_2. We were able to find the transition state (**5a(TS)**), which is shown in Figure 6. At the transition state, the Mülliken charges on the two hydrogens are 0.2099 and 0.2116, which differentiates them from one another. The more positive hydrogen atom leaves as a proton in the form of HCl, whereas the other hydrogen is retained on the ruthenium center, resulting in the formation of *trans*-$[Ru(H)(P(OH)_3)(H_2PCH_2CH_2PH_2)_2][OTf]$, **6**. This hydride complex is the common reaction product for all of the H−X (X = H, SiH_3, $H_2B{\cdot}PH_3$, and CH_3) bond activations and has an Ru−H bond distance of 1.632 Å, which is 0.188 Å shorter than the corresponding distance in the intermediate **5a**. The potential energy diagram with the energies of the intermediate **5a**, the transition state **5a-(TS)**, and the products with respect to the reactants (energy is taken as zero) is shown in Figure 7. The overall free energy change for the heterolytic cleavage of the H−H bond by the model complex **4** is 8.6 kcal/mol at the B3LYP/LANL2DZ and 11.04 kcal/mol at the BP86/ZORA/TZP level of theory. In dichloromethane, the transition state **5a(TS)** is more stabilized than the product. A similar result is obtained when both of the counterions are triflates. As can be seen, the barrier for the heterolysis of the H−H bond is low, which is consistent with our experiment wherein the heterolytic cleavage takes place even at 193 K in the presence of H_2 as a head gas. The mechanism of the heterolytic splitting of a coordinated dihydrogen and the effect of the counterions in the deprotonation of the dihydrogen complex *trans*-$[FeH(\eta^2\text{-}H_2)(dppe)_2]^+$ have been reported by Basallote and co-workers.[44]

Activation of the Si−H Bond. Silanes with at least one Si−H bond can bind to metal centers in an η^2-fashion. Theoretical calculations of the binding of H_2 and silanes (Si−H) to metal centers show similar characteristic features.[1a,45] Our calculations

(43) H−H distance = 0.7414 Å; source: *CRC Handbook of Chemistry and Physics*, 80th ed.; CRC Press: Boca Raton−Ann Arbor−Boston, 1999−2000.

(44) Basallote, M. G.; Besora, M.; Durán, J.; Fernández-Trujillo, M. J.; Lledós, A.; Máñez, M. A.; Maseras, F. *J. Am. Chem. Soc.* **2004**, *126*, 2320−2321.

(45) (a) Lin, Z. *Chem. Soc. Rev.* **2002**, *31*, 239−245. (b) Corey, J. Y.; Braddock-Wilking, J. *Chem. Rev.* **1999**, *99*, 175−292. (c) Schneider, J. J. *Angew. Chem., Int. Ed. Engl.* **1996**, *35*, 1068−1075. (d) Schubert, U. *Adv. Organomet. Chem.* **1990**, *30*, 151−187.

on the interaction of SiH_4 and the Ru-complex show that the intermediate **5b**, involved in the activation of the Si−H bond of SiH_4, consists of an η^1-silane. This is quite unique because we have not come across any example of η^1-silane complex in the literature so far. At the transition state **5b(TS)**, the metal-bound Si−H bond is stretched by 0.188 Å, as compared to a bond length of 1.483 Å for the other three Si−H bonds. Once again, the bond elongation is a modest 12.6%. The corresponding elongation at the BP86/ZORA/TZP level of theory is 17.1%. Heterolysis of the Si−H bond results in the formation of the ruthenium hydride complex **6**. The silylium cation $[H_3Si]^+$ interacts with the Cl^- counterion to give H_3SiCl as the other product. Consistent with the small activation barrier for the heterolysis of the Si−H bond in SiH_4 by the model complex **4** as seen from the potential energy diagram (Figure 7), the heterolytic cleavage of the Si−H bond in Et_3SiH and $EtMe_2$-SiH takes place at room temperature in a facile manner with no observable and/or isolable intermediates. The solvent dichloromethane does not have a significant effect on the reaction profile of the activation of Si−H bond.

Activation of the B−H Bond. On the basis of Shimoi's description of the nature of the bonding between borane adducts and electrophilic metal complexes,[34,35] we carried out theoretical studies on the binding and activation of the B−H bond in $H_3B{\cdot}PH_3$ using the model complex **4**. The optimized structure for the intermediate **5c** (Figure 6) shows that $H_3B{\cdot}PH_3$ interacts with the ruthenium through η^1-$HBH_2{\cdot}PH_3$. At the transition state **5c(TS)** (Figure 6), the length of the B−H bond that interacts with Ru is 1.441 Å. This bond is 0.241 Å longer than those of the non-interacting B−H bonds (1.2 Å). Thus, the η^1-B−H bond is elongated by 20% before undergoing cleavage. The remaining fragment of the borane, $[H_2B{\cdot}PH_3]^+$, interacts with the Cl^- counterion to give $ClH_2B{\cdot}PH_3$. The heterolysis of the B−H bond results in the formation of an Ru−H bond with a bond length of 1.736 Å. The fact that the B−H bond has to elongate by 20% (28% at the BP86/ZORA/TZP level) before undergoing heterolysis indicates that the process is facile at temperatures moderately higher than room temperatures. Consistent with the experimental result, the activation barrier in this case as well is small as seen in the potential energy diagram (Figure 7). The intermediate, **5c**, is more stabilized than the product in dichloromethane as compared to the gas-phase calculation.

Activation of the C−H Bond in Methane. Our efforts to heterolyze the C−H bond in methane afforded results that were not readily reproducible as discussed earlier. This prompted us to carry out the computational work. The inconsistency was especially disappointing because the H−H and the C−H bond energies are comparable. In addition, the B−H and the Si−H bonds could be activated using the same metal complex under similar reaction conditions. The failure to activate the C−H bond as compared to the Si−H can also stem from the different polarities of these bonds. The commonly encountered coordination mode of the three-center M−(η^2-H−CH_3) binding is perhaps not possible in **4** due to steric interactions. The intermediate structure **5d** (Figure 6) shows that methane interacts with the ruthenium through a C−H bond in an η^1-fashion. In the transition state (**5d(TS)**, Figure 6), the C−H bond undergoes elongation forming an Ru−H bond and the CH_3 fragment forming an incipient C−Cl bond with the counterion Cl^- at a distance of 2.463 Å. This transition state is higher in energy in relation to the other activation processes studied here (Figure 7), which is in tune with our inability to bring about the activation of CH_4 with the Ru complex despite repeated attempts. The bond distance of the C−H bond interacting with the ruthenium in **5d(TS)** is 1.657 Å, indicating an elongation by a whopping 0.575 Å as compared to that of the non-interacting C−H bonds (1.082 Å). At the transition state, the Ru−H distance is 1.720 Å and the C−Cl distance is 2.463 Å. Thus, the extent to which the C−H bond has to elongate (53.1%) before undergoing heterolysis is consistent with the high activation barrier for this process. This C−H bond elongation at the BP86/ZORA/TZP level of theory is 50.7%. The C−H bond elongation, in fact, is much larger than those of H−H, Si−H, and the B−H bonds for the heterolysis using model complex **4**. Similar to **5c**, the intermediate (**5d**) is also more stabilized than the product in dichloromethane as compared to the gas-phase calculation. A similar result was obtained when both of the counterions are triflates. Thus, the order of the bond elongation for these species follows: H−H < Si−H < B−H < C−H. A comparison of the transition states for the different activation processes given below brings in the inevitability of a high barrier for the C−H bond activation.

Comparison of the Potential Energy Surfaces for the Reaction of Model Complex 4 with H_2, SiH_4, $H_3B{\cdot}PH_3$, and CH_4. The potential energy profiles for the activation of H−X (X = H, SiH_3, $H_2B{\cdot}PH_3$, and CH_3) bonds by model complex **4** (Figure 7) show that the height of the activation barrier depends on several factors. The bond energies of H−X calculated at the same level of theory are 104.4, 86.7, 92.3, and 102.2 kcal/mol for H−H, H−SiH_3, H−$BH_2{\cdot}PH_3$, and H−CH_3 bonds, respectively. They match fairly well with the experimental values of 104.2, 90.3, and 104.8 kcal/mol, respectively, for H−H, H−SiH_3, and H−CH_3 bonds.[46] The experimental B−H bond energy in $H_3B{\cdot}PH_3$ is not available. The activation barriers for the heterolysis of the H−H, the Si−H, the B−H, and the C−H bonds are 8.6, 2.7, 17.7, and 57.5 kcal/mol, respectively. This indicates that the activation barrier depends not only on the H−X bond strength but also on other factors. The activation barrier does not depend in this case on the bond formed, but the overall energies of the reaction are influenced by this.[4b] The most dramatic aspect of these results is the very high barrier predicted for C−H bond activation of CH_4. H_2 with comparable bond energy has a much lower barrier. Musaev and Morokuma observed a barrierless H−H oxidative addition of H_2 to [Rh(Cp)(CO)] fragment, whereas a barrier of 6 kcal/mol was found for the same process for CH_4.[47] On the other hand, Conner et al. found that the intermolecular heterolytic activation of the H−H bond brought about by [Ru(NH_2)(CO)(PCP)] (PCP = 2,6-($CH_2P^tBu_2$)$_2C_6H_3$) was exoergic by 8.9 kcal/mol, whereas that of the C−H bond of methane was endoergic by 13.69 kcal/mol.[48]

The Ru−H distances calculated for the four intermediates, 1.820 (H_2, **5a**), 1.761 (SiH_4, **5b**), 1.811 ($H_3B{\cdot}PH_3$, **5c**), and 2.112 Å (CH_4, **5d**), already forebode the shape of things to come. The longest Ru−H distance of 2.112 Å is for the CH_4 complex, a result of the nonbonded H···H interactions; the C−H bond

(46) *CRC Handbook of Chemistry and Physics*, 72nd ed.; CRC Press: Boca Raton−Ann Arbor−Boston, 1991−1992.
(47) Musaev, D. G.; Morokuma, K. *J. Am. Chem. Soc.* **1995**, *117*, 799−805.
(48) Conner, D.; Jayaprakash, K. N.; Cundari, T. R.; Gunnoe, T. B. *Organometallics* **2004**, *23*, 2724−2733.

being very short cannot come very close to the Ru in the intermediate without extra steric interactions involving the remaining hydrogens of CH_4. Movement toward the transition state must decrease the Ru−H distances even further. The calculated Ru−H distances of 1.810 (H_2, **5a(TS)**), 1.728 (SiH_4, **5b(TS)**), 1.736 ($H_3B{\cdot}PH_3$, **5c(TS)**), and 1.720 Å (CH_4, **5d(TS)**) at the transition state are comparable to each other. However, to get to this range, the H of C−H bond had to traverse a longer path (2.112−1.720 Å) than for Si−H and B−H bonds. This increases the H···H nonbonded interactions, which is avoided by stretching the C−H bond to 1.657 Å, nearly breaking the C−H bond. This is a 53.1% elongation of the C−H bond from that of the parent CH_4. Naturally, the energy of the transition state is very high. Corresponding percentage increases are much smaller for $H-SiH_3$ (12.6%) and $H-BH_2{\cdot}PH_3$ (20%). This is because with this amount of the X−H stretch in the transition state the nonbonded interactions between the hydrogens on the phosphorus (of $H_2PCH_2CH_2PH_2$ ligand) and the remaining hydrogen on the Si and B atoms are within acceptable limits (2.4 Å, van der Waals radii of H_2). This is reflected in the nonbonded H···H distances: H···H = 2.448, 2.658 Å (**5d(TS)**); H···H = 2.646, 3.308 Å (**5b(TS)**); H···H = 2.320, 2.535 Å (**5c(TS)**). The C−H bond had to be stretched considerably to obtain these acceptable nonbonded distances, in comparison to B−H and Si−H. This is to be contrasted with the theoretical study on [Rh(Cp)(CO)] as the metal fragment.[48] The orientation of the Cp and the CO around the metal leaves ample room for the CH_4 to approach closely so that at the transition state the C−H bond need not be unduly stretched. The barrier is only 6 kcal/mol. This also points to the many parameters that have to be taken into account in designing ligands for X−H activation. The ligands where the steric interaction with the substituents on X has been taken care of are suitable for activating the C−H bond of CH_4.

Conclusions

The 16-electron, coordinatively unsaturated, dicationic ruthenium complex $[Ru(P(OH)_3)(dppe)_2][OTf]_2$ is "superelectrophilic" and activates the H−H (in H_2(g)), Si−H (in silanes), and B−H (in borane−Lewis base adducts) bonds in a heterolytic fashion. The common ruthenium-containing reaction product is the hydride complex *trans*-$[Ru(H)(P(OH)_3)(dppe)_2][OTf]$. The heterolytic activation of the C−H bond in methane using this ruthenium complex does not take place. The DFT calculations carried out at the B3LYP/LANL2DZ level using a model system $[Ru(P(OH)_3)(H_2PCH_2CH_2PH_2)_2][OTf][Cl]$ to get an insight into the variation in experimental reactivity showed that the activation barriers for the heterolysis of the H−H, the Si−H, and the B−H bonds are low, whereas that for the C−H bond is quite high. The high barrier in methane is due to the enormous stretching that the C−H bond has to undergo to avoid the unfavorable nonbonded H···H interactions.

Acknowledgment. Financial support from the Department of Science & Technology, India, and the Council of Scientific & Industrial Research, India, is gratefully acknowledged. We also thank the Department of Science & Technology, India, for funding the procurement of a 400 MHz NMR spectrometer under the "FIST" grant and the Supercomputer Education and Research Center, I.I.Sc., for computational facilities.

Supporting Information Available: NMR spectral stack plot, kinetic plots of the reaction of complex **1** with silanes, B3LYP/LANL2DZ-optimized structures of the free molecules and products, interaction diagram between H−H and metal fragments in **5a(TS)** from the ADF2005.01 program package, the total energies (au), zero point energies (kcal/mol), and the number of imaginary vibrational frequencies for the model structures **4**−**6**, XYZ coordinates and total energy (kcal/mol) of molecules at the B3LYP/LANL2DZ level of theory, BP86/ZORA/TZP-optimized structures of all molecules, and the complete ref 15. This material is available free of charge via the Internet at http://pubs.acs.org.

JA069044J